Available online at www.sciencedirect.com

ScienceDirect

Procedia CIRP 62 (2017) 281 – 286

www.elsevier.com/locate/procedia

10th CIRP Conference on Intelligent Computation in Manufacturing Engineering - CIRP ICME '16

Experimental study on fiber laser microcutting of Nimonic 263 superalloy

Silvio Genna[a,*], Flaviana Tagliaferri[b], Claudio Leone[a,c], Biagio Palumbo[b], Gaetano De Chiara[d]

[a]*CIRTIBS Research Centre, University of Naples Federico II, P.le Tecchio 80, 80125 Naples, Italy*
[b]*Department of Industrial Engineering, University of Naples Federico II, P.le Tecchio 80, 80125 Naples, Italy.*
[c]*Department of Industrial and Information Engineering, University of Campania, Via Roma 29, 81031 Aversa (Ce), Italy*
[d]*Avio Aero, Viale Giuseppe Luraghi 20, 80038 Pomigliano d'Arco (NA), Italy*

* Corresponding author. Tel.: +39 081 7682176; fax: +39 081 7682972. *E-mail address:* sgenna@unina.it

Abstract

Laser cutting of NIMONIC 263 sheet was investigated by using a 100 W Yb:YAG fiber laser. The study was divided in two phases. In the first one, the critical cutting speeds were found fixing the average power (80 W), changing the pulse duration, the cutting speed, the nozzle diameter and the focus position. Then, a full factorial design was adopted according to the DoE methodology. In order to determine which of the process parameters affect the kerf geometry and how, Analysis Of Variance (ANOVA) was used. Experimental results show the possibility to obtain kerf characterized by narrow width and low taper angle values.

Peer-review under responsibility of the scientific committee of the 10th CIRP Conference on Intelligent Computation in Manufacturing Engineering

Keywords: Laser microcutting; Fiber laser; Nimonic 263 superalloy; DoE, ANOVA

1. Introduction

Nowadays, laser technology is one of the most widely used manufacturing processes in material processing. This is thanks to its peculiar characteristics, such as: high precision, high flexibility, low thermal modifications and high productivity. This is particularly true especially when cutting or drilling are performed aerospace engine. In this components field, strict quality standard are required in terms tolerances and metallurgical characteristics (such as recast layer, oxides, etc.) perpendicular surfaces, no burr and no recast layer are required. High brilliance laser sources, such us fiber laser, allows to machine with reasonable precision most of the metallic materials.

The material removal rate (MRR) and the kerf geometry are functions of the process parameters, such as the type of adopted source (including wavelength, beam quality and beam spot dimension), the average power, the cutting speed, the focus position, the type of assistant gas and its pressure. Moreover, in case of pulsed laser sources, the MRR and kerf characteristics are also influenced by the pulse frequency, the pulse duration and the overlapping percentage. Consequently, the investigation of laser machining of aerospace materials is a topic in increasing interests. The effects of the process parameters on the kerf characteristics have been widely studied in the past. In [1-2] the influence of power and cutting speed in laser cutting of different steels adopting a CO_2 laser source, was studied. It was found that kerf width increases when the laser power increases and the cutting speed decreases. Moreover, in [1] it was found that the adoption of a reactive gas as assistant gas, instead of an inert gas, leads to a wider kerf and higher roughness. Also the focus position influences the kerf geometry; in [3] it was found that the minimum kerf width is obtained by setting the focus on the workpiece surface for thin sheets (< 1.5 mm) and inside the workpiece for thicker sheets (> 1.5 mm). In [4] a study on the influence of process parameters of Nd:YAG laser drilling of Ni-based superalloy sheet (1 mm in thickness) was presented. In the study, it was found that a spot overlap increase produces an enlargement of kerf, while a short pulse duration allows for a low kerf taper angle, if compared to a longer duration pulse. This results are consistent to what observed in similar studies on laser cutting of stainless steel [2, 5].

When Nd:YAG laser source were adopted, some negative effects, including micro-cracking, spatter, dross, and taper of the kerf were observed [4, 6-12]. Moreover, this kind of laser

Peer-review under responsibility of the scientific committee of the 10th CIRP Conference on Intelligent Computation in Manufacturing Engineering
doi:10.1016/j.procir.2016.06.109

sources often operated in low-order Gaussian modes and rarely in TEM_{00}. In comparison to that, the beam quality of a fiber laser is independent from the output power, over a wide range. This results in a better focussing and then higher cutting speeds with comparable or better kerf quality, in term of: small dimension, spatter and dross absence, recast layer and HAZ extension. Furthermore, these characteristics are enhanced by the use of high quality short and ultrashort pulsed laser [13-17]. However, when the material thickness is limited (< 1 mm), the use of a high quality fibre laser, working in CW or modulated regime, could be an economical and practical solution, as shown in [18-21].

In a previous paper [22], the possibility to have cuts characterised by a narrow kerf, low taper angle on Nimonic 236 sheet, 0.38 mm in thickness, was investigated by adopting a 100 W single-mode fibre laser. The results showed that an increase of the average power (by way of the on time) and of the gas pressure allowed to obtain regular kerfs, with no burrs. Consequently, in this work, the average power and the pressure were kept constant, while the pulse duration, the nozzle diameter and the position of the focusing lens were varied. A full factorial design was developed according to the Design of Experiments (DoE) methodology. The kerf geometry was measured by optical microscopy according to the UNI EN 12584 2001 and ISO 9013:2002 standard. The ANOVA was adopted to verify the influence of the process parameter on kerf geometry.

2. Equipment, material and experimental procedures

2.1. Equipment

The cutting tests were performed adopting a 100 W Fibre Laser (SPI-RedPower SP100C), working at the wavelength, $\lambda = 1090$ nm. The laser source is transferred via an optical fibre, 6 m in length, to a laser head (from HAAS LTI) mounted on a 3+1 axis CNC system. The laser source was controlled via an external laser controller (MCA LCT3001), which allows the setting of the power (from 10% to 100% maximum nominal power) and the regime: CW or modulated. In this last case it was also possible to set the pulse frequency and the pulse duration. The laser source power, the geometric patterns and the beam speed were controlled by the CNC system.

Table 1 shows the detailed characteristics of the laser system.

2.2. Material

The investigated material was the Nimonic 263® (UNS N07263/W. Nr. 2.4650) in form of rolled sheets 0.38 mm in thickness.

Nimonic 263 was developed by Rolls-Royce (1971) Ltd. to provide a sheet material which offer improved properties in terms of proof stress and creep strength. The chemical composition and the main properties of Nimonic 263 are reported in [22]. This material is often adopted in the combustion chamber of aeronautical engine.

Table 1. Laser source characteristics (SPI -RedPower SP100C).

Parameters	Value	Unit
Wavelength	1090	[nm]
Nominal power	100	[W]
Mode operation	CW or Modulated	--
Pulse frequency	1-18	[kHz]*
Pulse duration	1-0.01 ms	[ms]*
Beam diameter ($1/e^2$)	5.0 ± 0.5	[mm]
Full angle divergence	<0.4	[mrad]
Beam Quality	TEM_{00} (M^2 <1.1)	--
	BPP 0.38	[mm.mrad]
Beam expander	0.32 x	--
Focal length	50	[mm]
Beam diameter at the focal spot	$\phi \approx 48$	[μm]

* in modulated regime

2.3. Experimental procedure

The study was divided in two phases. In the first one, the critical cutting speeds, defined as the speed beyond which it is not possible to cut the sheet, were found. For this purpose, linear cuts were performed fixing the average power (80 W), the pressure and the type of the assistant gas (12 bar and Nitrogen) and the stand-off distance (0.2 mm) while varying beam travel speed, the pulse duration, the nozzle diameter (0.5 and 1 mm) and the position of the focusing lens (the beam was focused on the surface, (0 mm position) and 0.2 mm inside the sheet.

Then, the second phase a tests was performed to verify the influence of the process parameters on the kerf geometry. Linear cuts 40 mm long were performed at 90% of the critical cutting speed found in the first experimental phase. A full factorial design was developed according to the Design of Experiments (DoE) methodology [23].

The control factors were the following: pulse duration (D), focus position (F) and nozzle diameter (N). In order to determine which of the process parameters affect the kerf geometry and how, ANalysis Of VAriance (ANOVA) was adopted.

The control factors were selected on the bases of a previous work [22]. In particular the average power and the pressure were kept constant, near at the maximum values settable on the machine (80 W and 12 bar, respectively), while the pulse duration, the nozzle diameter (0.5 and 1 mm) and the position of the focusing lens (on the surface and inside the sheet) were varied. Table 2 summarizes the levels of control factors and their settings. Four replications for each treatment (i.e. process condition) were performed, resulting in a total of 64 experimental runs. The replications of each treatment were performed to provide more consistent response repeatability. To reduce the disturbance of any unconsidered noise factor, the order of trials was randomized both in the treatments and in their replications.

After the tests, part of the samples were cut, included in epoxy resin and then polished using abrasive paper of grit size up to P2500 (Standard ISO 6344). Then, images of the kerf sections were taken by an optical microscope (Zeiss

Axioskop 40), and the geometry was measured according to the UNI EN ISO 12584 and ISO 9013 standard. In particular, the kerf width at the inlet of the beam (upper kerf or Uk), and at the exit of the beam (bottom kerf or Bk), the taper angle (Ta) and the perpendicularity (u) were measured.

Fig. 1 shows a scheme of the kerf section and how Uk, Bk, Ta and u were measured.

3. Experimental results and discussion

3.1. Critical cutting speed

In Fig. 2 critical cutting speed (Ccs) as a function of duration for two different nozzle diameters (0.5 and 1 mm) is reported. Ccs depends on nozzle diameter (N) and duration (D). In particular it increases as D increases. Moreover its highest values are achieved when the smaller nozzle is adopted. T

he cutting speeds adopted in the second experimental phase are the 90% of the Ccs, for each nozzles diameter. In Fig. 2 the dashed lines represent the adopted cutting speeds (Cs) (Cs = 90% Ccs).

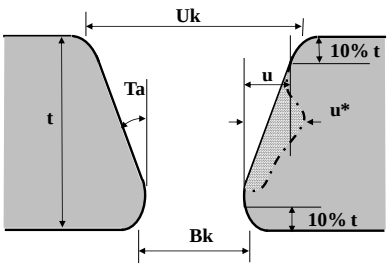

Fig. 1. Definition of kerf geometry parameters (UNI EN 12584 and ISO 9013): upper kerf (Uk); bottom kerf (Bk), taper angle (Ta) and perpendicularity (u).

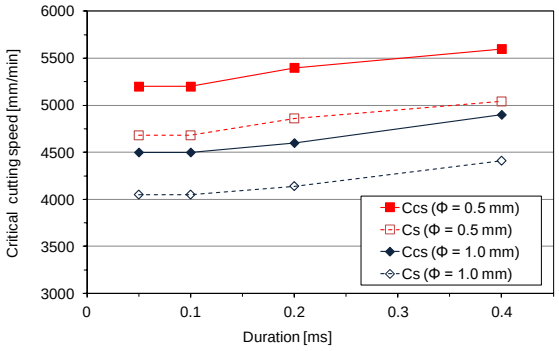

Fig. 2. Critical cutting speed as a function of duration for different nozzle diameters. The dashed lines represent the adopted cutting speeds (Cs = 90% Ccs).

3.2. Statistical analysis of results

The ANalysis Of VAriance (ANOVA) assumes that the observations are normally and independently distributed with the same variance for each treatment or factor level. Before the analysis, these assumptions have been successfully checked via analysis of residuals, in agreement with what reported in [23-25]. However, these results were not reported here for sake of briefness. The ANOVA results are summarized in Table 3 in terms of *p*-values. Assuming a 95 % confidence level ($\alpha = 0.05$), a control factor, or a combination of control factors, is statistically significant if the *p*-value is less than 0.05.Focus position (F) influences all the response variables except for the bottom upper kerf. The nozzle diameter affects all the response variables except for the perpendicularity. At last the pulse duration (D) influences only the taper angle. Regarding the two way interaction, ANOVA indicates, as significant, the interaction F*R, that affects all the response variables, and the interaction F*D, only for the taper angle.

3.3. Technological interpretation

Fig.s 3-4 depict some kerf sections with focus position on the surface (F = 0 mm) and inside the sheet (F = 0.2 mm), respectively, for different nozzle diameters (N) and pulse durations (D). From this figures, it is clear appears, is the presence of a decrease of kerf width occurring when a the largest nozzle is adopted (N = 1 mm). Moreover, the profile inside the kerf appears more regular when the pulse duration (D) increases.

The main effects plots and the interaction plots are reported in Figs. 5-8. In the main effects plots (Figs. 5-6) the significant factors are highlighted by continuous lines. In the interaction plots (Figs.. 7-8) only the statistically significant interactions are reported. Furthermore, the vertical bars denote 0.95 confidence intervals. In Fig. 5a the upper kerf decreases moving the focus position from the surface (F = 0 mm) to inside the sheet (F = 0.2 mm); it decreases changing the nozzle diameter from 0,5 mm to 1 mm.

Table 2. Control factors and their levels

Control factor	1	2	3	4	Unit
Pulse duration, *D*	0.05	0.10	0.20	0.4	[ms]
Focus position, *F*	0	-	-	0.2	[mm]
Nozzle diameter, *N*	0.5	-	-	1.0	[mm]

Table 3. Result of ANOVAin terms of p-value. The significant control factors (p-value < 0.05) are highlighted by bold and underlined text.

Source	Uk [µm]	Bk [µm]	Ta [°Deg]	u [µm]
F [mm]	**0.019**	0.413	**0.002**	**0.020**
N [mm]	**0.000**	**0.000**	**0.003**	0.817
D [ms]	0.367	0.054	**0.002**	0.232
F*N	**0.009**	0.363	**0.000**	**0.002**
F*D	0.188	**0.008**	**0.028**	0.412
N*D	0.129	0.733	0.214	0.250

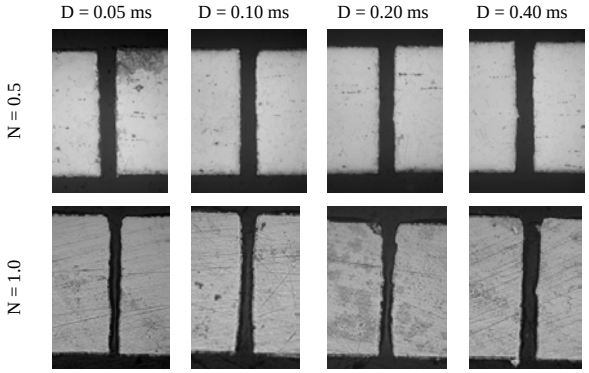

Fig.3. Images of the kerf sections with focus position on the surface (F=0 mm) for different nozzle diameters (N) and pulse durations (D).

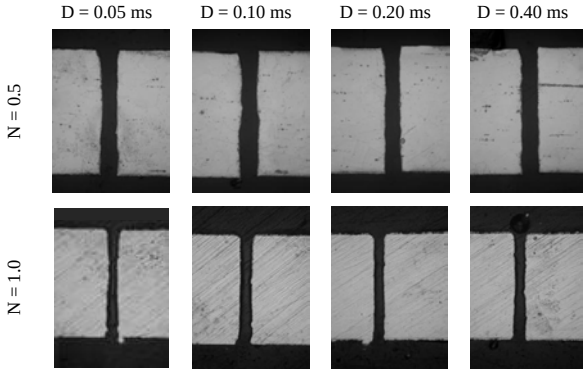

Fig. 4. Images of the kerf sections with focus position inside the thickness (F=0.2 mm) for different nozzle diameters (N) and pulse durations (D).

The first phenomenon can be explained taking into account that, when the beam focus is inside the material, the area irradiated on the surface increases, but, since the laser is a single-mode source, the Gaussian tails contributions do not exceed the energy threshold of processing.

Consequently, a decrease of Uk is expected. The effect of the use of larger nozzle (N = 1 mm) can be explained considering that the function of assistant gas is to blow the molten material away from the cutting area. Therefore, when the larger nozzle is adopted (i.e. the gas speed and the drag force are lower) the removing of the molten materials is less effective, so, a reduction of Uk occurs. Similar effect results for Bk, as shown in Fig. 5b. The taper angle (Ta) decreases moving the focus position from the surface (F = 0) to inside the sheet (F = 0.2); it increases changing the nozzle diameter (N) from 0,5 mm to 1 mm. Moreover, taper angle (Ta) has its maximum value when the smallest pulse duration is adopted (D = 0.05 ms). The Ta behaviour is directly influenced by Uk and Bk. So, its performance is the result of the two variables behaviour: when the focus moves from the surface to inside the sheet, Uk decreases and, therefore, Ta decreases.

On the other hand, when the diameter nozzle changes from 0 mm to 1mm, both the kerf widths decrease in different way causing an increasing Ta.

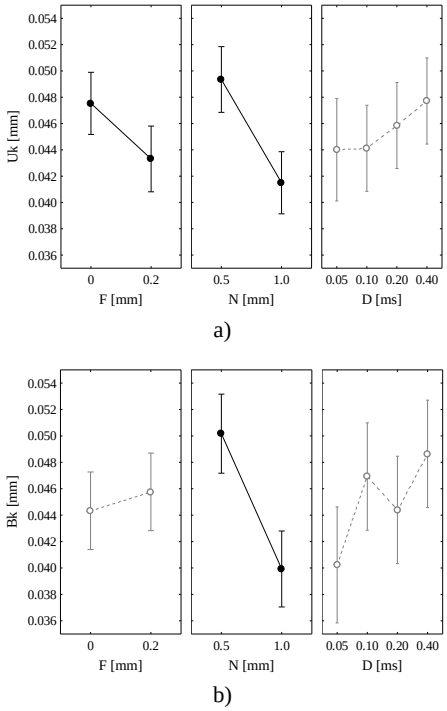

Fig. 5. Main effects plots for a) upper kerf (Uk); b) bottom kerf (Bk). Vertical bars denote 0.95 confidence intervals.

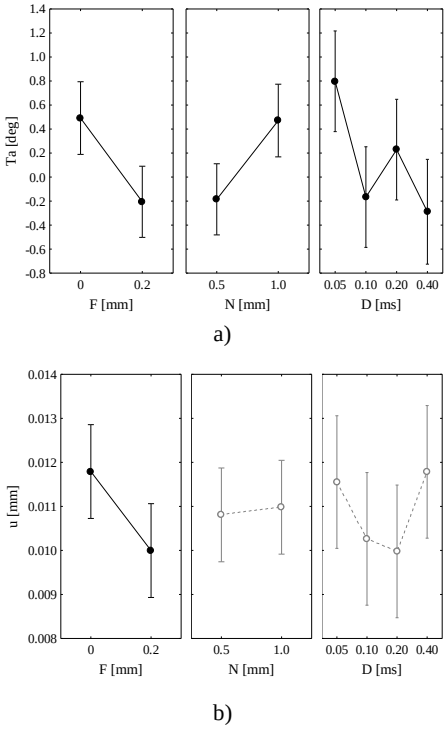

Fig. 6. Main effects plots for a) taper angle (Ta); b) perpendicularity (u). Vertical bars denote 0.95 confidence intervals.

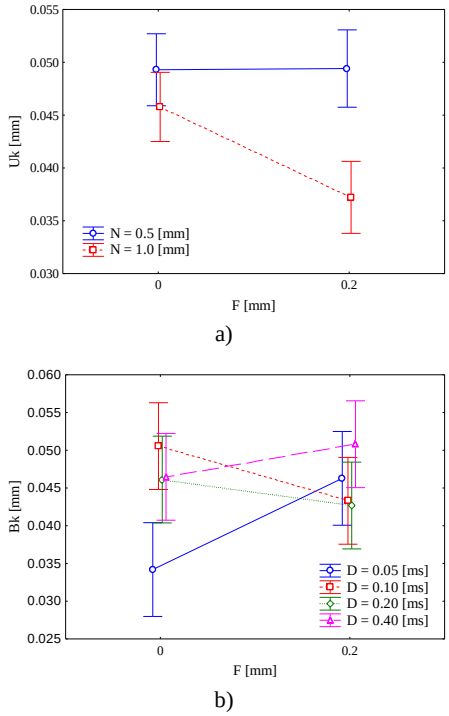

Fig. 7. Interaction plots for a) upper kerf (Uk); b) down kerf (Bk). Vertical bars denote 0.95 confidence intervals.

An increase of the duration results in an increasing interaction time, thus when the duration is high (D = 0.4 ms) a more regular kerf is obtained, and so a reduction of Ta occurs.

The opposite occurs for D = 0.05 ms. Fig. 6b shows the main effect of perpendicularity (u); it decreases when the focus position passes from the surface to inside the sheet. This happens because, when the focus is placed inside the sheet, a reduction of the energy density occurs on the surface and an increase of the energy density on the exit of the kerf is obtained. In these conditions a more regular kerf is obtained.

The interaction F*N is due to the low peak power (i.e. 100 W); under this condition the irradiance is low and the cutting process does not involve vaporisation. As result, the molten material removal from the kerf is due to gas action that is more efficient when smaller nozzle diameter is adopted. This phenomenon is not manifested for Bk.

The interaction D*F is mainly due to the low level of duration (D = 0.05 ms). In this condition, when the focus is placed on the surface (F = 0 mm), the duration is just enough to melt the material in all its thickness. So, when the focus is pleased inside the sheet (F = 0.2 mm), the energy density at the exit of the kerf increases and an enlargement of Bk (and than a decreasing of Ta) occurs.

This phenomenon is not manifested for Bk.

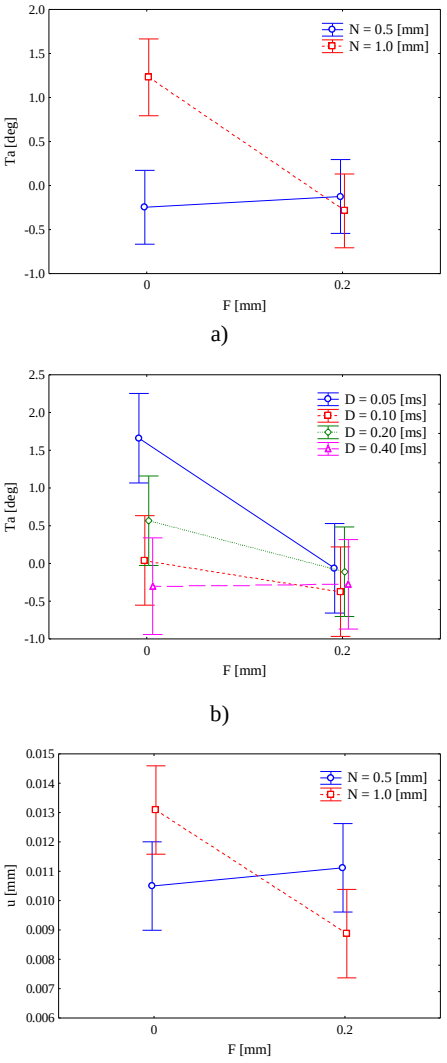

Fig. 8. Interaction plots for a) b) taper angle (Ta); c) perpendicularity (u). Vertical bars denote 0.95 confidence intervals.

Conclusions

In this work, laser microcutting tests were performed on 0.38 mm-thick Nimonic 263 sheets, adopting a 100 W single mode fibre laser, to study the influence of the process parameters on the kerf geometry. From the results, the main conclusions are the following:

- the operating window was defined. Under the adopted conditions, the critical cutting speed depend on the pulse duration and nozzle diameter, it varies in the range 4000 ÷ 5500 mm/min;
- the bottom kerf is affected only by the nozzle diameter, while the upper kerf by focus position and nozzle;
- the perpendicularity u is affected only by the focus position while the taper angle by all the control factors; the

optimum taper angle is with the focus placed 0.2 mm below the surface;

- the molten material removal from the kerf is due to gas action that is more efficient when the little nozzle is adopted.

It is worth noting that the kerf widths, the tolerance and the taper angle are compatible to the requirements for the cutting and drilling operation on the effusion cooling system placed inside the turbine blade.

Acknowledgements

The present work was supported by the "*Ministero dello Sviluppo Economico*" of Italy as part of the PON-FIT research program. Grant No. B01/0707/01-03/X17 which is gratefully acknowledged.

This work has been developed within the research line "Statistics, QUAlity and REliability" (SQUARE) of the Joint Laboratory "Interactive DEsign And Simulation" (IDEAS) between the University of Naples Federico II (Italy) and the Fraunhofer Institute for Machine Tools and Forming Technology IWU of Chemnitz (Germany).

The authors are also grateful to Avio Aero for providing the material adopted in the experimentation.

References

[1] Lamikiz A, Lacalle LNL, Sanchez JA, Pozo D, Etayo JM, Lopez JM, CO_2 laser cutting of advanced high strength steels (AHSS), Applied Surface Science, 2005; 242: 362-368.

[2] Rajaram N, Ahmad, JS, Cheraghi SH, CO_2 laser cut quality of 4130 steel, Int. International Journal of Machine Tools and Manufacture, 2003; 43: 351-358.

[3] Karatas C, Keles O, Uslan I, Usta Y, Laser cutting of steel sheets: influence of workpiece thickness and beam waist position on kerf size and striation formation, Journal of Materials Processing Technology, 2006; 172: 22-29.

[4] Thawari G, Sarin Sundar JK, Sundararajan G, Joshi SV. Influence of process parameters during pulsed Nd:YAG laser cutting. of nickel-base superalloys. Journal of Materials Processing Technology 2005; 170: 229-239.

[5] Araújo D, Carpio FJ, Méndez D, García AJ, Villar MP, García R, Jiménez D, Rubio L, Microstructural study of CO_2 laser machined heat affected zone of 2024 aluminum alloy, Applied Surface Science, 2003; 208-209/1: 210-217.

[6] Leone C, Genna S, Caggiano A, Tagliaferri V, Molitierno R, An investigation on Nd:YAG laser cutting of Al 6061 T6 alloy sheet, Procedia CIRP, 2015; 28: 64-69.

[7] Leone C, Genna S., Caggiano A, Tagliaferri V, Molitierno R, Influence of process parameters on kerf geometry and surface roughness in Nd:YAG laser cutting of Al 6061 T6 alloy sheet, in press on International Journal of Advanced Manufacturing Technology, 2016; 87/9: 2745-2762.

[8] Dubey AK, Yadava V. Multi-objective optimization of Nd:YAG laser cutting of nickel-based superalloy sheet using orthogonal array with principal component analysis. Optics and Lasers in Engineering 2008; 46: 124-132.

[9] Rao R, Yadava V. Multi-objective optimization of Nd:YAG laser cutting of thin superalloy sheet using grey relational analysis with entropy measurement. Optics and Lasers in Engineering. 2009; 41: 922-930.

[10] Sibalija TV, Petronic SZ, Majstorovic VD, Prokic-Cvetkovic R, Milosavljevic A. Multi-response design of Nd:YAG laser drilling of Ni-based superalloy sheets using Taguchi's quality loss function. multivariate statistical methods and artificial intelligence. International Journal of Advanced Manufacturing Technology. 2011; 54/5-8: 537-552.

[11] Petronić S, Kovačević G, Milosavljević A, Milosavljević A, Sedmak A. Microstructural changes of Nimonic-263 superalloy caused by laser beam action. Physica Scripta. 2012; T149. Article number 014080.

[12] Morace RE, Leone C, De Iorio I. Cutting of thin metal sheets using Nd:YAG lasers with different pulse duration. *Proceedings of SPIE*. 2005; 6157: art. no.61570Q.

[13] Dausinger F. Precise drilling with short pulsed lasers. Proceedings of SPIE. 2000; 3888: 180-187

[14] Arnaboldi S, Bassani P, Biffi CA, Carnevale M, Lecis N, Lo Conte A, Previtali B, Tuissi A. Microcutting of niticu alloy with pulsed fiber laser. Biennial Conference on Engineering Systems Design and Analysis. ASME-ESDA 2010. 12-14 July 2010. Instanbul Turkey. 1: 593-602

[15] Biffi CA, Previtali B. Spatter reduction in nanosecond fibre laser drilling using an innovative nozze. Int J. Advanced Manufacturing Technology. 2013; 66: 1231-1245.

[16] Kling R, Dijoux M, Romoli L, Tantussi F, Sanabria J, Mottay E. Metal micro drilling combining high power femtosecond laser and trepanning head. Proceedings of SPIE. 2013; 8608: Article number 86080F.

[17] Romoli L, Rashed CAA, Fiaschi M. Experimental characterization of the inner surface in micro-drilling of spray holes: A comparison between ultrashort pulsed laser and EDM. Optics and Laser Technology. 2014; 56: 35-42.

[18] Baumeister M, Dickmann K, Hoult T. Fiber laser micro-cutting of stainless steel sheets. Applied Physics A: Materials Science and Processing. 2006; 85/2: 121-124.

[19] Astarita A, Genna S, Leone C, Memola Capece Minutolo F, Paradiso V, Squillace A. Ti-6Al-4V Cutting by 100W fibre laser in both CW and modulated regime. Key Engineering Materials. 2013; V. 554-557: 1835-1844.

[20] Lutey AHA, Fortunato A, Ascari A, Carmignato S, Leone C, Laser Cutting of Lithium Iron Phosphate Battery Electrodes: Characterization of Process Efficiency and Quality, Optics & Laser Technology, 2015; 65: 164-174.

[21] Leone C, Genna S, Tagliaferri V, Fibre Laser Cutting of CFRP Thin Sheets by Multi-Passes Scan Technique, Optics and Lasers in Engineering, 2014;53: 43-50.

[22] Genna S, Leone C, Palumbo B, Tagliaferri F, Statistical Approach to Fiber Laser Microcutting of NIMONIC® C263 Superalloy Sheet Used in Effusion Cooling System of Aero Engines, Procedia CIRP, 2015; 33: 521-526.

[21] Montgomery DC. Design and Analysis of Experiments. New York. Wiley. 2008.

[24] Leone C, Genna S, Tagliaferri F, Palumbo B, Dix M, Experimental investigation on laser milling of aluminium oxide using a 30W Q-Switched Yb:YAG fiber laser. Optics & Laser Technology, 2016; 76/22: 127-137.

[25] Tagliaferri F, Dittrich M, Palumbo B, A systematic approach to Design of Experiments in Waterjet Machining of High Performance Ceramics, as chapter of book: Management and Industrial Engineering, Davim: Design of Experiments in Production Engineering, Springer, 2015.